REPORT DOCUMENTATION PAGE

Form Approved
OMB No. 0704-0188

1. REPORT DATE *(DD-MM-YYYY)*	**2. REPORT TYPE**	**3. DATES COVERED** *(From - To)*
07-11-2013	Journal Article	September 2012- November 2012

4. TITLE AND SUBTITLE

How to drive CARS in reverse

5a. CONTRACT NUMBER
FA8650-08-D-6930

5b. GRANT NUMBER

5c. PROGRAM ELEMENT NUMBER
0602202F

6. AUTHOR(S)

Brett H. Hokr, Gary D. Noojin, Georgi I. Petrov, Hope Beier, Robert J. Thomas, Benjamin A.
Rockwell, and Vladislav V. Yakovlev

5d. PROJECT NUMBER
7757

5e. TASK NUMBER
HD

5f. WORK UNIT NUMBER
04

7. PERFORMING ORGANIZATION NAME(S) AND ADDRESS(ES)

Air Force Research Laboratory
Human Effectiveness Directorate
Bioeffects Division
Optical Radiation Bioeffects Branch
4141 Petroleum Rd
JBSA Fort Sam Houston, TX 78234

TASC
4241 Woodcock Dr
San Antonio, Texas 78228

8. PERFORMING ORGANIZATION REPORT NUMBER

9. SPONSORING / MONITORING AGENCY NAME(S) AND ADDRESS(ES)

Air Force Research Laboratory
Human Effectiveness Directorate
Bioeffects Division
Optical Radiation Bioeffects Branch
4141 Petroleum Rd
JBSA Fort Sam Houston, TX 78234

10. SPONSOR'S/MONITOR'S ACRONYM(S)

711 HPW/RHDO

11. SPONSOR'S/MONITOR'S REPORT NUMBER(S)

AFRL-RH-FS-JA-2013-0007

12. DISTRIBUTION / AVAILABILITY STATEMENT

Approved for public release (PA); distribution unlimited. PA Case No: TSRL-PA-13-0064

13. SUPPLEMENTARY NOTES

14. ABSTRACT

Remote chemically specific detection of trace impurities in the atmosphere from distances on the order of kilometers is an important problem from both an environmental and a national defense viewpoint. A new scheme is discussed consisting of the remote generation of a backward propagating stimulated Raman pulse. This pulse is then used to drive a coherent anti-Stokes Raman scattering scheme, resulting in a strong chemically specific signal propagating back to the detector.

15. SUBJECT TERMS

16. SECURITY CLASSIFICATION OF:			**17. LIMITATION OF ABSTRACT**	**18. NUMBER OF PAGES**	**19a. NAME OF RESPONSIBLE PERSON**
Unclassified					Semih Kumru
a. REPORT	**b. ABSTRACT**	**c. THIS PAGE**			**19b. TELEPHONE NUMBER** *(include area code)*
Unclassified	Unclassified	Unclassified	U	5	

Standard Form 298 (Rev. 8-98)
Prescribed by ANSI Std. Z39.18

Journal of Modern Optics, 2013
http://dx.doi.org/10.1080/09500340.2013.846428

Taylor & Francis
Taylor & Francis Group

How to drive CARS in reverse

Brett H. Hokr[a,b,c*], Gary D. Noojin[c], Georgi I. Petrov[b], Hope T. Beier[d], Robert J. Thomas[d], Benjamin A. Rockwell[d] and Vladislav V. Yakovlev[b]

[a]*Department of Physics & Astronomy, Texas A&M University, College Station, TX, USA;* [b]*Department of Biomedical Engineering, Texas A&M University, College Station, TX, USA;* [c]*TASC Inc., San Antonio, TX, USA;* [d]*Air Force Research Labs, Ft. Sam, Houston, TX, USA*

(*Received 1 March 2013; accepted 14 September 2013*)

Remote chemically specific detection of trace impurities in the atmosphere from distances on the order of kilometers is an important problem from both an environmental and a national defense viewpoint. A new scheme is discussed consisting of the remote generation of a backward propagating stimulated Raman pulse. This pulse is then used to drive a coherent anti-Stokes Raman scattering scheme, resulting in a strong chemically specific signal propagating back to the detector.

Keywords: remote sensing; stimulated Raman scattering; coherent anti-Stokes Raman scattering; backward CARS; remote light source

1. Introduction

Continuous monitoring of trace agents in the atmosphere, out to distances on the order of kilometers, is a challenging but important endeavor with applications ranging from monitoring pollution to an early warning system for chemical and biological weapons [1]. Currently, light detection and ranging (LIDAR) is the best technique available. However, LIDAR suffers greatly from relying on the isotropic scattering of an outgoing probe beam in the air. This weak signal leads to a lack of sensitivity or long integration times, severely limiting the practical range of such devices. Coherent scattering, such as coherent anti-Stokes Raman scattering (CARS), offers the possibility of obtaining a large spectroscopic signal from trace amounts of gas. However, in order to have a backward propagating CARS signal, a backward propagating pump or probe beam is required to satisfy the phase matching conditions. Hence, to use this powerful spectroscopic technique, we must first generate a spatially coherent backward propagating light source remotely at distances on the order of kilometers.

Recently, several schemes have been proposed to remotely generate a spatially coherent backward propagating pulse. The first uses the impurities in air as a lasing medium [2]. Two photon pumping or Raman pumping utilizes two different color pulses to pump these impurities at a controllable distance. The dispersion of air allows the pump pulses to overlap at a distance determined by a relative initial delay between the pulses. A swept-gain geometry scheme is then used to preferentially amplify the spontaneous emission in the backward direction to overcome the low gain per length due to the low density of these impurities.

Another proposal for generating backward propagating light is to use an intense ultraviolet pulse focused at a predefined distance to two photon dissociate molecular oxygen, and subsequently pump atomic oxygen by two-photon absorption into a three-level lasing scheme [3,4]. This scheme has the ability to produce a backward propagating infrared pulse at 845 nm and has been experimentally observed on a small scale in the lab in ambient air [5,6].

Furthermore, a different method involving lasing in atmospheric nitrogen has also been proposed [3,7]. This scheme uses a femtosecond pulse to create a filament at a specified distance by using a temporal prechirp. A high power nanosecond laser follows and 'heats' this plasma creating an electron avalanche, analogous to the electric discharge used in traditional nitrogen lasers.

These schemes are all viable sources of remotely generated bright spatially coherent light. However, the impurities and nitrogen lasing methods require multiple high power lasers to be accurately synchronized, greatly increasing the cost and difficulty. The oxygen scheme will suffer from substantial absorption from ozone at 226 nm, making it difficult to deliver sufficient pumping power at kilometer scale distances. To avoid the problems associated with a multiple laser set up and gain the freedom of tunability to minimize atmospheric absorption, we propose to use stimulated Raman scattering (SRS) in either oxygen or nitrogen to generate a bright backward propagating light source [8].

*Corresponding author. Email: brett.hokr@tamu.edu

SRS has been experimentally observed in high pressure gas cells filled with both nitrogen and oxygen [9–14]. However, a backward propagating SRS signal in ambient air has not yet been observed in the lab.

2. Discussion

Stimulated Raman scattering, like stimulated emission, can generate a bi-directional signal provided the gain length is short compared to the spatial pulse length and the Rayleigh length. The stimulated Raman gain coefficient is given by

$$G = \frac{\Delta N}{\hbar c^2 \pi^2 n_S^2 \nu_S^2 \nu_p \delta\nu_S} \frac{\partial\sigma}{\partial\Omega}, \tag{1}$$

where ΔN is the population density (containing any thermal distributions of states) of the species leading to the gain, n_s is the refractive index at the Stokes frequency, ν_s is the frequency (cm^{-1}) of the scattered radiation, ν_p is the pump frequency, and $\delta\nu_s$ is the frequency width of the scattered light [14]. To a good approximation, the Raman cross-section, $\partial\sigma/\partial\Omega$, is given by

$$\frac{\partial\sigma}{\partial\Omega} = A \frac{\nu_S^4}{\left(\nu_i^2 - \nu_p^2\right)^2}, \tag{2}$$

where A and ν_i are empirical fitting parameters that have been experimentally measured for the major constituents of air [15]. The Raman gain coefficient is plotted in Figure 1 for atmospheric nitrogen and oxygen at sea level. For Figure 1, we used the cross-section data measured in [15], the line width data given in [14], and the atmospheric data presented in [16], but we note the lack of consistency amongst tabulated measurements for many of these parameters, some differing by an order of magnitude. Regardless, in both nitrogen and oxygen, there is a substantially larger Raman gain if we work in the ultraviolet.

Recently, an experiment was attempted in ambient air using the 4th harmonic of a picosecond seeded Nd:YAG laser. The output pulses were ~ 10 mJ 30 ps pulses at 266 nm with a 10 Hz repetition rate. These pulses were focused into ambient air using a 35 cm focal length fused silica lens. Unfortunately, before we were able to reach the SRS threshold, we observed optical breakdown of the air.

Using these experimental parameters and neglecting the breakdown of air, the total gain factor was $GI_pz \sim 19$, where I_p is the intensity of the pump pulse, and z is the propagation distance. Because we are discussing backward SRS the propagation distance was taken to be the shorter of one half the spatial pulse length or twice the Rayleigh length. In the geometry above, twice the Rayleigh length is shorter, but only by a factor of two. Traditionally, threshold is defined to be when the total gain factor exceeds approximately 30. If we are able to avoid thermal breakdown using a different geometry, we are close to threshold. When planning future experiments, it will be important to keep in mind that extending the Rayleigh length significantly beyond the length of the pulse will be detrimental since our peak intensity will suffer from a larger focal spot, while our interaction distance will be limited by the length of the pulse itself. In order to optimize the effect, one should select a focusing geometry such that the Rayleigh length and the spatial pulse length are similar.

It is a possibility that our experiment was not sensitive to stimulated rotational Raman scattering (SRRS). SRRS has been shown to have a lower threshold value in atmospheric air [17–20], but with a small frequency shift (71 cm^{-1} in oxygen and 75 cm^{-1} in nitrogen) [14] it is very difficult to

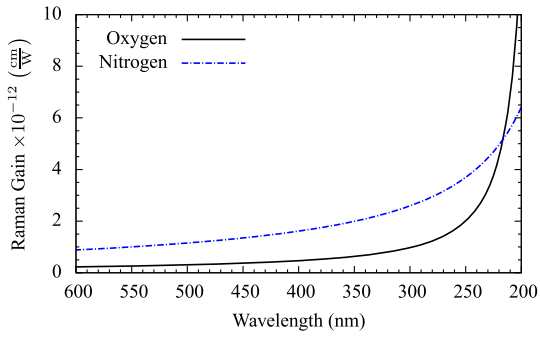

Figure 1. Raman gain coefficient for atmospheric oxygen and nitrogen using Equation (1) and numerical values given in Ref. [14–16]. For the number density we have assumed that all of the population is in the ground state. (The color version of this figure is included in the online version of the journal.)

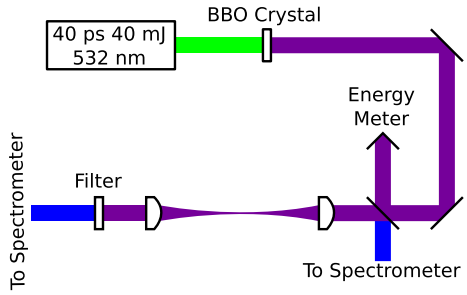

Figure 2. Schematic of the attempted experiment. A ~ 40 ps 532 nm pulse is frequency doubled into a ~ 30 ps 266 nm, which is then focused into ambient air. (The color version of this figure is included in the online version of the journal.)

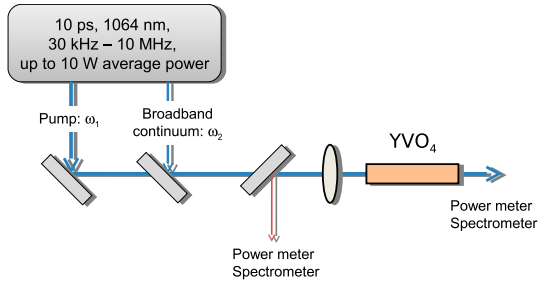

Figure 3. Schematic of the experimental setup used for backwards CARS experiment. (The color version of this figure is included in the online version of the journal.)

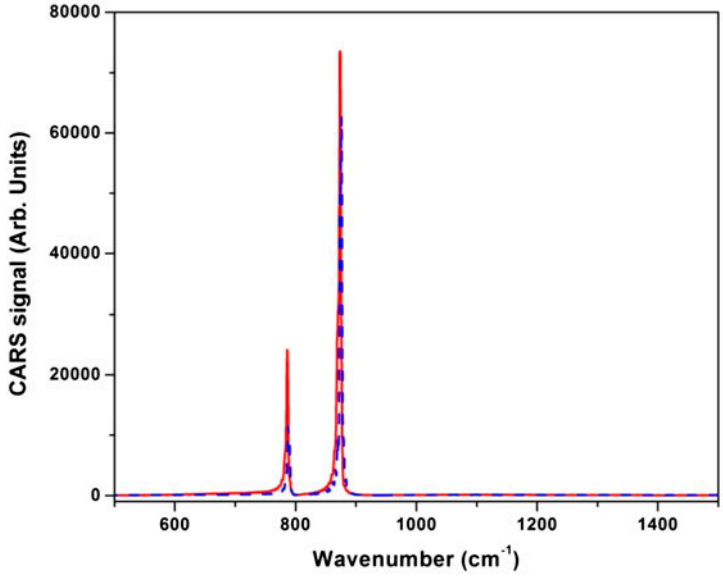

Figure 4. Backward (red solid line) and forward (dashed blue line) CARS signals generated in the 25-mm-long YVO_4 crystal. The forward propagating signal was attenuated 20 times to fit the scale. The data acquisition time was 50 ms, and the CARS signal's amplitude is expressed in the number of counts. (The color version of this figure is included in the online version of the journal.)

distinguish from the pump light. To distinguish the backward SRRS signal, we propose moving the beam splitter shown in Figure 2 behind the lens and removing the forward propagating detection optics. Thus, any strong signal that is reflected by the beam splitter could only come via some coherent backward scattering mechanism.

To facilitate backward CARS generation, one would clearly benefit from having a process, which does not have a threshold intensity, i.e. can be accomplished even at relatively low incident intensities. We note that in atmosphere or any other environment where remote sensing is needed, elastic light scattering is always present. If we send two intense light beams, the pump at frequency ν_p and the Stokes at frequency ν_S, in such a way that the difference frequency is in resonance with some molecular vibration, for example the 2335 cm^{-1} line of the nitrogen molecule, the process of Raman gain occurs. If the Stokes beam experiences elastic scattering, it will be amplified both in the forward and backward direction. If we just focus on the backward propagating Stokes beam, which was just amplified by a strong pump beam, it will generate a strong CARS signal using the following four-wave mixing process: $\nu_{\mathrm{CARS}} = \nu_p - \nu_S^+ + \nu_S^-$, with the phase-matching condition for k-vectors results in $k_{\mathrm{CARS}} = k_p - k_S^+ + k_S^-$. Here, $(+)$ denotes forward propagating waves and $(-)$ denotes backward propagating fields. This results in a backward propagating beam at the pump frequency. This beam can participate in another four-wave mixing process, $\nu'_{\mathrm{CARS}} = \nu_p - \nu_S^+ + \nu_S^-$, where the propagation vector will be pointing in the backward direction. If a broadband Stokes beam is sent together with a narrowband pump beam, a broadband CARS scheme [21–23] can be realized leading to the simultaneous remote detection of the full Raman spectrum.

To demonstrate a proof of principle, we used a 25-mm long YVO_4 crystal (Crystech, Inc.), which is known to have a strong Raman cross-section [24]. We employed the same set-up used in Ref. [23], but instead of a microscope objective, an aspheric focusing lens (FL = 30 mm, ThorLabs, Inc.) was used to focus pump and Stokes beam inside the YVO_4 crystal. The forward propagating CARS signal was re-collimated using an identical aspheric lens and through a short-pass filter and directed into the spectrometer (Andor, Inc.) with the attached deep-depletion thermoelectrically cooled CCD (Andro, Inc.) for the broadband signal detection. The backward propagating CARS signal was collected through the same focusing lens, and after a short-pass filter was directed to the second detection channel of the above-mentioned spectrometer. This experimental setup is depicted in Figure 3. With as little as 200 mW input pump power (pulse repetition rate was set at 100 kHz) on both the pump and supercontinuum radiation (as the Stokes beam), both the forward- and backward- propagating CARS signals are clearly seen, as is shown in Figure 4. The forward propagating signal was attenuated by a factor of 20 using a set of neutral density filters to scale with the back-propagating signal. The two strongest Raman peaks (see Ref. [24] for details) clearly overlap in the CARS spectra. We confirmed that the back-propagating signal was well collimated, which was easy to see at slightly higher intensities when this beam was clearly visible on the IR-sensitive card. This demonstrates a proof-of-principle, that such back-propagating CARS signal generation can be accomplished.

3. Conclusion

A full scheme for the remote detection of trace impurities in the atmosphere using stimulated Raman scattering to drive a backward CARS process is discussed and proof of principle experiments are shown. Given the preliminary nature of these experiments, we emphasize the observation, for the first time, of a backscattered collimated CARS signal by re-amplifying the back-propagating scattering beam from the medium using Raman process in the medium itself.

Acknowledgements

The authors acknowledge the Texas A&M Supercomputing Facility (http://sc.tamu.edu/) for providing computing resources useful in conducting the research reported in this paper.

Funding

This work was partially supported by National Institutes of Health Grant R21EB011703 and National Science Foundation Grants ECCS-1250360, DBI-1250361, and CBET-125036.

References

[1] Arora, R.; Petrov, G.I.; Yakovlev, V.V.; Scully, M.O. *Proc. Natl. Acad. Sci. U.S.A.* **2012**, *109* (4), 1151–1153.
[2] Kocharovsky, V.; Cameron, S.; Lehmann, K.; Lucht, R.; Miles, R.; Rostovtsev, Y.; Warren, W.; Welch, G.; Scully, M.O. *Proc. Natl. Acad. Sci. U.S.A.* **2005**, *102* (22), 7806–7811.
[3] Hemmer, P.R.; Miles, R.B.; Polynkin, P.; Siebert, T.; Sokolov, A.V.; Sprangle, P.; Scully, M.O. *Proc. Natl. Acad. Sci. U.S.A.* **2011**, *108* (8), 3130–3134.
[4] Yuan, L.; Hokr, B.H.; Traverso, A.J.; Voronine, D.V.; Rostovtsev, Y.; Sokolov, A.V.; Scully, M.O. *Phys. Rev. A* **2013**, *87*, 023826.
[5] Dogariu, A.; Michael, J.B.; Scully, M.O.; Miles, R.B. *Science* **2011**, *331* (6016), 442–445.
[6] Traverso, A.J.; Sanchez-Gonzalez, R.; Yuan, L.; Wang, K.; Voronine, D.V.; Zheltikov, A.M.; Rostovtsev, Y.; Sautenkov, V.A.; Sokolov, A.V.; North, S.W.; Scully, M.O. *Proc. Natl. Acad. Sci. U.S.A.* **2012**, *109* (38), 15185–15190.
[7] Sprangle, P.; Peñano, J.; Hafizi, B.; Gordon, D.; Scully, M. *Appl. Phys. Lett.* **2011**, *98* (21), 211102–211102.
[8] Maier, M.; Kaiser, W.; Giordmaine, J. *Phys. Rev.* **1969**, *177* (2), 580.
[9] Lempert, W.R.; Zhang, B.; Miles, R.B.; Looney, J.P. *J. Opt. Soc. Am. B* **1990**, *7* (5), 715–721.
[10] Hagenlocker, E.E.; Rado, W.G. *Appl. Phys. Lett.* **1965**, *7* (9), 236–238.
[11] Everall, N.; Partanen, J.; Barr, J.; Shaw, M.J. *Opt. Commun.* **1987**, *64* (4), 393–397.
[12] Alekseyev, V.; Grasiuk, A.; Ragulsky, V.; Sobel'Man, I.; Faizulov, F. *IEEE J. Quantum. Electron.* **1968**, *4* (10), 654–656.
[13] Chatelet, M.; Oksengorn, B. *Chem. Phys. Lett.* **1975**, *36* (1), 73–75.
[14] Martin, W.; Winfield, R. *Appl. Opt.* **1988**, *27* (3), 567–577.
[15] Bischel, W.; Black, G. *AIP Conf. Proc* **1983**, *100*, 181–187.
[16] *U.S. Standard Atmosphere, 1976*; U.S. Government Printing Office: Washington, DC, **1976**.
[17] Rokni, M.; Flusberg, A. *IEEE J. Quantum. Electron.* **1986**, *22* (7), 1102–1108.
[18] Herring, G.; Dyer, M.J.; Bischel, W.K. *Opt. Lett.* **1986**, *11* (6), 348–350.
[19] Henesian, M.; Swift, C.; Murray, J.R. *Opt. Lett.* **1985**, *10* (11), 565–567.
[20] Averbakh, V.; Makarov, A.; Talanov, V.I. *Quantum Electron.* **1978**, *8* (4), 472–476.
[21] Yakovlev, V. *J. Raman Spectrosc.* **2003**, *34* (12), 957–964.
[22] Arora, R.; Petrov, G.I.; Yakovlev, V.V. *J. Mod. Opt.* **2008**, *55* (19–20), 3237–3254.
[23] Arora, R.; Petrov, G.I.; Liu, J.; Yakovlev, V.V. *J. Biomed. Opt.* **2011**, *16* (2), 021114.
[24] Yakovlev, V.V.; Petrov, G.I.; Zhang, H.F.; Noojin, G.D.; Denton, M.L.; Thomas, R.J.; Scully, M.O. *J. Mod. Opt.* **2009**, *56*, 1970–1973.